(*E*)−(*Z*) Selectivity in the Polymerization of 2-Butene Promoted by Ni(II) Brookhart-Type Catalysts

Giuseppe Milano, Gaetano Guerra, Mina Mazzeo, Claudio Pellecchia, and Luigi Cavallo*

Dipartimento di Chimica, Università di Salerno, Via Salvador Allende, I-84081 Baronissi (SA), Italy

Received August 5, 2004; Revised Manuscript Received November 5, 2004

ABSTRACT: We offer a rationalization of the different reactivity observed in the polymerization of (*E*)- and (*Z*)-2-butene isomers with (α-diimine)Ni(II) complexes, known as "Brookhart catalysts". Quantum mechanics calculations suggest that the two isomers of 2-butene coordinate similarly to the metal and that the slower reactivity of the (*Z*) isomer is related to stronger steric interactions at the transition state for insertion into the Ni−chain bond. The similar coordination energies suggested that the presence of the (*Z*) isomer should not inhibit reactivity of the (*E*) isomer. This point was confirmed with polymerization experiments performed with a 40% (*Z*)-2-butene:60% (*E*)-2-butene mixture.

Introduction

In the past decade, complexes based on late transition metals were proved effective catalysts in the polymerization of ethene and, with reduced activity, of propene.[1−3] These discoveries opened alternative routes to the polymerization of monoalkenes based on early transition metals, Ti and Zr in particular.[4,5]

As occurred for group 4 catalysts, the new systems were tested also in the polymerization of more complicated monomers. Brookhart and Leatherman used (α-diimine)Ni(II) complexes such as those of Chart 1, the so-called "Brookhart catalysts", in the polymerization of an internal olefin, namely 2-butene.[6] These polymerization studies resulted in a somewhat surprising behavior. First, the NMR spectra of the obtained homopolymers are consistent with a highly regioregular polymer with a $-CH_2-CH_2-CH(CH_3)-$ repeat unit. Although methyl branches are predominant, minor amounts of ethyl branches were also observed. Methyl and ethyl branches in the resulting polymers were easily rationalized in terms of chain-walking mechanisms, which were also used to explain methyl branches in the polymerization of ethene.[7−10]

Second, and yet unexplained, only the (*E*)-2-butene isomer was able to react with the Ni-based catalysts, leading to high molecular mass polymeric materials, whereas reaction of the precatalysts **1a**−**b** with the (*Z*)-2-butene isomer led to isolation of no polymer products. Finally, it was also observed that the nature of the substituents on the aryl rings and the backbone structure of the diimine ligand have a strong influence on the activity of the catalysts.[6]

Herein, we offer a possible explanation of the different reactivites of the (*E*)- and (*Z*)-2-butene isomers as well as of the different activities of catalysts such as those based on **1a** and **2**. To this end, we utilized a theoretical approach based on quantum mechanics/molecular mechanics (QM/MM) techniques.[11,12] We already performed a similar analysis in the case of ethene/2-butene copolymerization with group 4 C_2 and C_s symmetric metallocenes. We only recall that we predicted the (*Z*)-2-butene isomer to be more reactive with C_2 symmetric metallocenes, while the (*E*)-2-butene isomer to be more reactive with C_s symmetric metallocenes. These predictions were confirmed by experiments.[13,14]

Chart 1

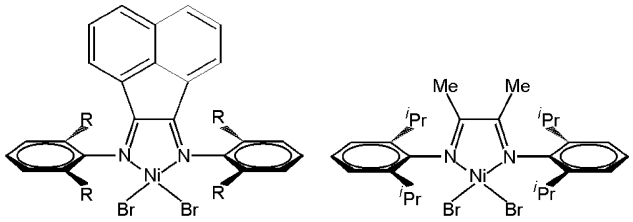

1a R = Me
1b R = *i*-Pr

2

In the present paper we investigate the two reactions illustrated in Scheme 1. In the first step we calculate the energy of coordination of the monomers (both isomers of 2-butene) using a solvent-coordinated species as the resting state. The solvent molecule was modeled with a single benzene molecule π-coordinated to the metal. After solvent displacement, the transition state for insertion into the Ni−(growing chain) bond was considered.

The *n*-propyl group was used to simulate a growing chain as that obtained from chain-straightening pro-

Scheme 1

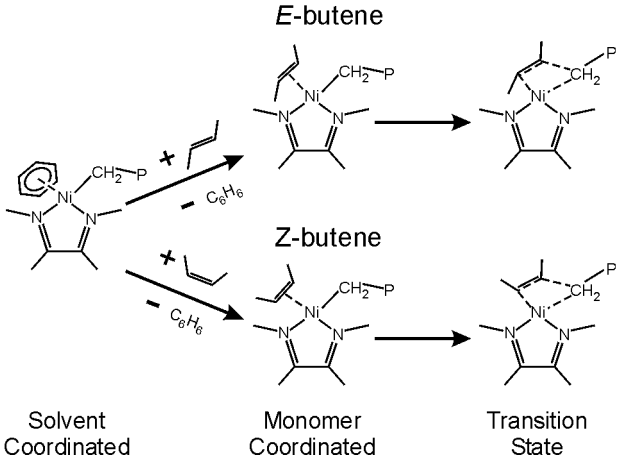

* Corresponding author. E-mail: lcavallo@unisa.it.

10.1021/ma048373y CCC: $30.25
Published on Web 02/16/2005

Table 1. Energies of the Monomer Coordinated Intermediates and of the Transition States for Insertion Relative to the Solvent Coordinated Intermediates[a]

	1a		**2**	
	(*Z*)	(*E*)	(*Z*)	(*E*)
solvent coordinated	0.0	0.0	0.0	0.0
monomer coordinated	−12.8	−13.7	−6.2	−6.5
transition state	2.3	−5.7	6.1	2.2
barrier to insertion	15.1	8.0	12.2	8.6

[a] The insertion barriers, $\Delta E^{\ddagger}$, calculated as the energy difference between the transition states and the monomer coordination intermediates are also reported. All the energies are in kcal/mol.

cesses, which are believed to occur almost regularly after monomer insertion, in the case of polymerization of internal olefins. The approach here considered allowed us to avoid the discussion of unrealistic gas-phase coordination energies (roughly 20−30 kcal/mol) for reactions that, instead, occur in solution. For each reaction, the solvent-coordinated intermediate is assumed as reference state at zero energy.

Results and Discussion

The negative energies reported in Table 1 for the monomer coordinated intermediates indicate that for both isomers of 2-butene, and for both catalysts **1a** and **2**, the monomer is able to displace the solvent molecule from the metal. However, the sharply more negative values in the case of the systems based on **1a** indicate that this kind of ligand substitution reaction is much more favored when the aryl rings of the diimine are substituted with small Me groups. In this case, the small 2-butene molecule can coordinate effectively to the metal atom. Instead, in the case of system **2**, the bulky *i*-Pr groups prevent an easy access to the metal also to 2-butene. As to a comparison between the two isomers of 2-butene, with both **1a** and **2** the (*E*) isomer coordinates better than the (*Z*) isomer by less than 1 kcal/mol. The substantially similar coordination energies indicate that the different reactivity of the two monomers is not related to a different coordination ability.

Turning our attention to the transition states, note that with both **1a** and **2** the transition states for insertion of the (*E*) isomer into the Ni−(*n*-propyl) bond is at lower energy relative to the corresponding transition state for insertion of the (*Z*) isomer. Considering that at the level of the coordination intermediates there were no substantial energy differences between the two isomers, it is not surprising that the activation barriers for insertion of the (*E*) isomer are remarkably lower than those for insertion of the (*Z*) isomer. The preference for the (*E*) isomer, calculated as the difference between the insertion barrier of the (*Z*) and (*E*) isomers, is somewhat stronger for **1a** (7.1 kcal/mol) than for **2** (3.6 kcal/mol). Nevertheless, in both cases our findings are in good qualitative agreement with the experimental data.[6]

To understand the origin of this difference, the transition states for (*E*)- and (*Z*)-2-butene insertion into the Ni−C(*n*-propyl) bond of systems based on **2** are shown in parts A and B of Figure 1, respectively. In both structures the C_β and the following atoms of the growing chain are oriented farther away from the methyl group on the C atom of butene that is going to form the new C−C bond. The transition state for (*E*)-2-butene insertion presents only few short distances between the methyl groups of the (*E*)-2-butene molecule and the ligand. These interactions occur between the C atom marked by a star in Figure 1A and C atoms of the nearby aromatic ring of the diimine ligand marked by black spheres. Differently, the transition state for (*Z*)-2-butene insertion is characterized by several short distances between the methyl groups of the (*Z*)-2-butene molecule and the ligand. These interactions occur between the C atom marked by a star in Figure 1B and the C atoms of the nearby aromatic ring of the diimine ligand marked by black spheres.

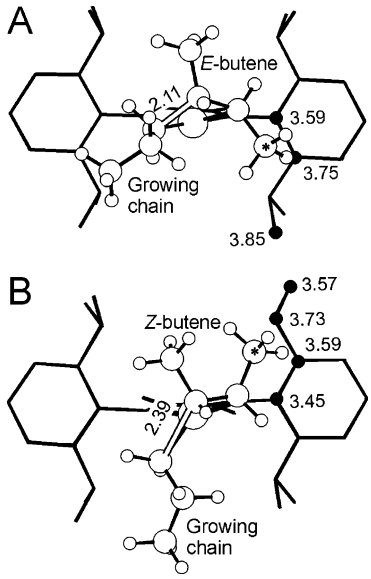

Figure 1. QM/MM transition states for insertion of the (*E*) and (*Z*) isomers of 2-butene into the Ni−C σ bond, parts A and B, respectively. Short distances between the carbon atoms marked by a ∗ and the carbons atoms marked by a ● are indicated in Å.

Table 2. 2-Butene Polymerization Data[a]

	catalyst	monomer	time (h)	yield (g)	branches × 1000 C
1	**1a**	(*E*)-2-butene	2	1.07	243
2	**1a**	60%(*E*)-2-butene/ 40% (*Z*)-2-butene	2	0.60	243
3	**1a**	(*Z*)-2-butene	2	traces	
4	**1a**	(*Z*)-2-butene	12	0.40	219
5	**1b**	(*Z*)-2-butene	12	0.06	202
6	**2**	(*Z*)-2-butene	12		

[a] Reaction conditions: 15 mL of toluene, 2×10^{-5} mol of catalyst, 4 mL of MMAO/heptane solution, 1.4 g of 2-butene, temperature 25 °C.

The steric pressure related to (*Z*)-2-butene insertion is also evidenced by larger distortions in the coordination geometry at the metal atom. To quantify this distortion, we take the angle formed by the Ni−C_α bond with the N−Ni−N plane. While in the transition state for (*E*)-2-butene insertion this angle is 9°, in the transition state for (*Z*)-2-butene insertion is 37°. In the latter case, this deviation also results in a remarkably puckered Cossee-like four-center transition state (see Figure 1B).

As final remark, we note that the coordination intermediates corresponding to coordination of the two butene isomers are of substantially similar energy. This suggests that the less reactive (*Z*) isomer should not prevent polymerization of the more reactive (*E*) isomer. This is in reasonable qualitative agreement with the experimental findings of Table 2, which indicate that reasonable polymerization activity is obtained also in the case of a mixture of both isomers in the composition feed.

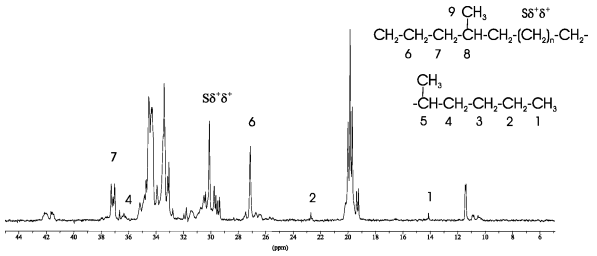

Figure 2. ^{13}C NMR spectrum of polymer of (*Z*)-2-butene obtained by **1a**, corresponding to run 3 of Table 2.

The ability of the models to predict the behavior of the two isomers in polymerization reaction is confirmed by experimental results of selected 2-butene polymerization tests reported in Table 2. In agreement with theoretical analysis, when polymerization experiments are performed with a 40% (*Z*)-2 butene:60% (*E*)-2 butene mixture (entry 2), the presence of the less reactive (*Z*) isomer does not inhibit the polymerization of the more reactive (*E*) isomer: the yield and the microstructure (243 branches per 1000 carbon atoms) of the polymer obtained are the same as the product achieved by the pure (*E*) isomer under similar polymerization conditions.

This is somewhat different from the case of 2-butene/ethylene copolymerization with C_s symmetric metallocenes. In that case the less reactive (*Z*) isomer coordinates better than the more reactive (*E*) isomer, resulting in a reduced reactivity of the (*E*) isomer when a mixture of both isomers was used in the feed.[13,14] About the reactivity of (*Z*)-2-butene, Brookhart reported that no polymeric products have been isolated upon reaction with precatalysts **1a** and **1b** and the pure (*Z*) monomer. Our theoretical studies evidencing higher but not prohibitive activation barriers for (*Z*) isomer insertion suggested us to investigate the reactivity of this isomer in polymerization reactions. Under polymerization conditions similar to those used for the (*E*) isomer, we obtained polymeric products using either **1a** and **1b** catalysts (entries 3 and 4). The ^{13}C NMR spectrum of the polymer obtained with **1a** is shown in Figure 2. In addition to the main resonances described by Brookhart for (*E*)-2-butene polymers, signals related to isolated methyl groups[15] and $S\delta^+\delta^+$ carbon atoms are also observed. The more complex microstructure can be again explained in terms of the above-mentioned chain-walking isomerization mechanism, but in this case, a reduced rate of insertion for the (Z) isomer allow successive isomerizations of the growing chain (β-hydride eliminations followed by reinsertions) before that a new subsequent monomer insertion occurs. The reduced rate of insertion relative to the rate of chain isomerization causes, coherently, a decrease of the polymer molecular weight confirmed by weak resonances corresponding to *n*-alkyl end groups detectable in the ^{13}C NMR spectrum.[16]

A substantial analogue microstructure is observed for polymer achieved by the more encumbered catalyst **1b**, but a less elevated percentage of branches (202 per 1000 carbon atoms) consistent with more frequent isomerization phenomena is observed. No polymeric products are obtained upon reaction with precatalyst **2**.

It is also worth noting that in the case of system **1a**, bearing the less bulky Me groups on the aryl rings of the ligand, the transition state for (*E*)-butene insertion is at lower energy relative to the solvent coordinated species, which implies that monomer insertion is more favored than monomer dissociation. With the bulkier system **2**, the transition state for (*E*)-butene insertion is at higher energy relative to the solvent-coordinated species, which implies that monomer dissociation is more favored than monomer insertion. This can be related to the different steric pressure of the aryl rings and the backbone structure of the diimine ligand and is in qualitative agreement with the much higher TOF experimentally observed for systems such as **1a** relative to the TOF of systems such as **2**.[6]

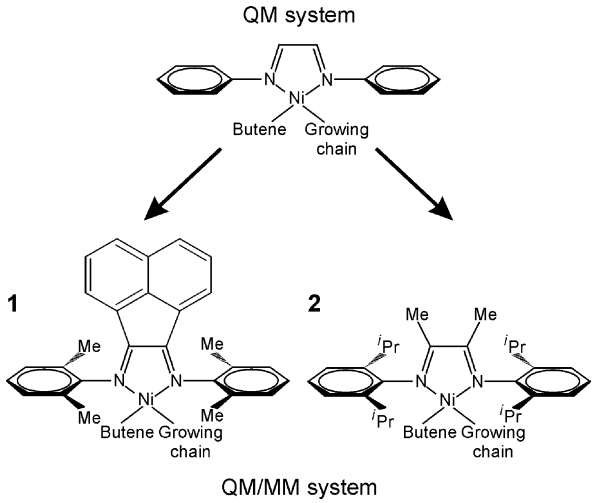

Figure 3. Schematic representation of the partitioning of the QM/MM systems into QM and MM parts.

Conclusions

In this paper we presented a rationalization of the different reactivity observed in the polymerization of (*E*)- and (*Z*)-2-butene isomers with (α-diimine)Ni(II) complexes. Our quantum mechanics calculations indicate that (1) selectivity between the two isomers of 2-butene does not originate at the coordination step, since they coordinate similarly to the metal, and (2) selectivity is instead predicted at the transition for insertion into the Ni−chain bond. In the case of the (*Z*) isomer, the geometry of the transition state is characterized by several short distances between one methyl group of the monomer and the nearby N-bonded aryl group of the ligand. In agreement with the theoretical predictions, our experimental results indicate that (1) polymerization of the (*E*) isomer is not inhibited by the presence of the (*Z*) isomer and (2) although with low activity, the (*Z*) isomer can be polymerized with catalysts **1a** and **1b**.

Computational Details

Stationary points on the potential energy surface were calculated with the ADF package.[17] A triple-ζ STO basis set was used for Ni, while double-ζ STO basis sets, augmented by one polarization function, were used for N and C (2s, 2p) and H (1s). For the QM part of the energy we used a density functional approach based on the BP86 level of theory.[18−20] The partitioning of the systems into QM and MM parts only involves the diimine ligand and is illustrated in Figure 3. Precisely, the Me and the *i*-Pr substituents on the aromatic rings, and the methyl and naftyl groups on the bridges of **1** and **2**, respectively, were included in the MM part. The CHARMM force field was used in the MM calculations.[22] This approach has been validated in previous studies.[13,23−27]

Experimental Details

General. 2-Butene monomers were purchased from Aldrich and used without further purification. A solution of modified methylaluminoxane (MMAO) in heptane (d = 0.73 g/mL) containing 23−27% isobutyl groups was purchased from Akzo Nobel. Toluene was refluxed over sodium diphenylketyl for 48 h and distilled under nitrogen before use. Precatalysts **1** and **2** were synthesized according to literature procedures.[28]

Polymerization Procedure. Polymerizations were performed by introducing 10 mL of anhydrous toluene and 4 mL of MMAO into a 100 mL reactor equipped with a magnetic stirrer. 1.4 g of 2-butene was condensed in the solution, previously thermostated to −78 °C and placed under vacuum. Successively, the solution was backfilled with nitrogen and thermostated at the desired polymerization temperature; at this point an appropriate precatalyst slurry (0.02 mmol) in toluene (5 mL) was added using a syringe. Polymerizations were stopped by the addition of methanol acidified with HCl. The precipitated polymers were recovered by filtration, dried (80 °C, vacuum oven, overnight), and weighed.

Characterization. ^{1}H and ^{13}C NMR spectra were recorded on a Bruker Advance 400 MHz spectrometer operating a 298 K. The samples were prepared by dissolving 30 mg of polymer in $CDCl_3$ in a 5 mm o.d. tube. The spectra were referenced vs TMS using the solvent residual resonance as internal chemical shift reference. The number of branches was quantified by ^{1}H NMR spectroscopic analysis of the polymer.

Note Added in Proof. After this manuscript was accepted for publication, a mechanistic study of cis and trans-2-butene polymerization catalyzed by a strictly analogous Pd(III) catalyst was published (Liu, W.; Brookhart, M. *Macromolecules* **2004**, *23*, 6099). Our prediction that the different reactivity of the two isomers of 2-butene is related to different insertion barriers is in excellent agreement with the main conclusion of the Liu and Brookhart paper.

Acknowledgment. This work was supported by the MURST of Italy (Grants PRIN 2004 and FISR 1999), Università di Salerno (Fondo Piccole Apparecchiature 2002), and Basell Polyolefins.

Supporting Information Available: Cartesian coordinates of all the structures discussed; ^{1}H and ^{13}C NMR spectra of polymers. This material is available free of charge via the Internet at http://pubs.acs.org.

References and Notes

(1) Ittel, S. D.; Johnson, L. K.; Brookhart, M. *Chem. Rev.* **2000**, *100*, 1169.
(2) Mecking, S. *Angew. Chem., Int. Ed.* **2001**, *40*, 534.
(3) Gibson, V. C.; Spitzmesser, S. K. *Chem. Rev.* **2003**, *103*, 283.
(4) Brintzinger, H.-H.; Fischer, D.; Mülhaupt, R.; Rieger, B.; Waymouth, R. M. *Angew. Chem., Int. Ed. Engl.* **1995**, *34*, 1143.
(5) Resconi, L.; Cavallo, L.; Fait, A.; Piemontesi, F. *Chem. Rev.* **2000**, *100*, 1253.
(6) Leatherman, M. D.; Brookhart, M. *Macromolecules* **2001**, *34*, 2748.
(7) Johnson, L. K.; Killian, C. M.; Brookhart, M. *J. Am. Chem. Soc.* **1995**, *117*, 6414.
(8) Svejda, S. A.; Johnson, L. K.; Brookhart, M. *J. Am. Chem. Soc.* **1999**, *121*, 10634.
(9) Gates, D. P.; Svejda, S. A.; Onate, E.; Killian, C. M.; Johnson, L. K.; White, P. S.; Brookhart, M. *Macromolecules* **2000**, *33*, 2320.
(10) Leatherman, M. D.; Svejda, S. A.; Johnson, L. K.; Brookhart, M. *J. Am. Chem. Soc.* **2003**, *125*, 3068.
(11) Maseras, F.; Morokuma, K. *J. Comput. Chem.* **1995**, *16*, 1170.
(12) Woo, T. K.; Cavallo, L.; Ziegler, T. *Theor. Chim. Acta* **1998**, *100*, 307.
(13) Guerra, G.; Longo, P.; Corradini, P.; Cavallo, L. *J. Am. Chem. Soc.* **1999**, *121*, 8651.
(14) Longo, P.; Grisi, F.; Guerra, G.; Cavallo, L. *Macromolecules* **2000**, *33*, 4647.
(15) De Pooter; M.; Smith; P. B.; Dohrer, K. K.; Bennet, K. F.; Meadows, M. D.; Smith; C. G.; Scouwenaars, H. P.; Geerards, R. A. *J. Appl. Polym. Sci.* **1991**, *42*, 399.
(16) Hayashy, T.; Inoue, Y.; Chûjô, R.; Asakura, T. *Macromolecules* **1988**, *21*, 2675.
(17) *ADF 2002, User's Manual*; Vrije Universiteit of Amsterdam, Amsterdam: The Netherlands.
(18) Becke, A. D. *J. Chem. Phys.* **1993**, *98*, 1372.
(19) Becke, A. D. *J. Chem. Phys.* **1993**, *98*, 5648.
(20) Perdew, J. P. *Phys. Rev. B* **1986**, *33*, 8822.
(21) Perdew, J. P. *Phys. Rev. B* **1986**, *34*, 7406.
(22) Brooks, B. R.; Bruccoleri, R. E.; Olafson, B. D.; States, D. J.; Swaminathan, S.; Karplus, M. *J. Comput. Chem.* **1983**, *4*, 187.
(23) Deng, L.; Woo, T. K.; Cavallo, L.; Margl, P. M.; Ziegler, T. *J. Am. Chem. Soc.* **1997**, *119*, 6177.
(24) Milano, G.; Cavallo, L.; Guerra, G. *J. Am. Chem. Soc.* **2002**, *124*, 13368.
(25) Milano, G.; Fiorello, G.; Guerra, G.; Cavallo, L. *Macromol. Chem. Phys.* **2002**, *203*, 1564.
(26) Cavallo, L.; Solà, M. *J. Am. Chem. Soc.* **2001**, *123*, 12294.
(27) Jacobsen, H.; Cavallo, L. *Chem. Eur. J.* **2001**, *7*, 800.
(28) tom Diek, H.; Svoboda, M.; Greiser, T. *Z. Naturforsch., B: Chem. Sci.* **1981**, *36*, 823.

MA048373Y